Journal of Hydroscience and Hydraulic Engineering
Vol. 5, No. 1, July, 1987, pp.27-37.

A TURBULENCE-BASED EXPRESSION FOR THE ENTRAINMENT COEFFICIENT FOR TWO-LAYERED STRATIFIED FLOWS

By

Masaru Ura,

Department of Civil Engineering, Kyushu Institute of Technology, Tobataku Kitakyushu 804, Japan

Toichiro Tsubaki,

Department of Civil Engineering, Nagasaki University, Nagasaki 852

Nobuhiro Matsunaga and Tadashi Namikawa

Department of Civil Engineering Hydraulics and Soil Mechanics, Kyushu University, Fukuoka 812, Japan

SYNOPSIS

An investigation has been undertaken of stably stratified two-layer flows where one layer with fully developed turbulence entrains non-turbulent fluid of the second layer. The velocity of entrainment has been measured for four types of two-layered flows and analyzed on the basis of the view that the turbulence plays an essential role in the entrainment process. These flows involve turbulence generated by an oscillating-grid, by shear flow of an upper-layer and by wind-induced flows with and without surface waves. The turbulence intensity and integral lengthscale have been chosen as characteristic quantities of the turbulence, and the density difference between the two fluids as an effective buoyancy. These quantities form a non-dimensional parameter, a local Richardson number Ri. A coefficient of entrainment E is defined as the ratio of the entrainment velocity to the turbulence velocity, and the analysis yields the empirical expression $E = 0.7\ Ri^{-3/2}$ when $5.0 \lesssim Ri \lesssim 5.0 \times 10^2$. The agreement of this equation with the data from diverse experiments indicates that the process of entrainment depends closely on turbulence in this range of Ri.

INTRODUCTION

Estimations of entrainment velocity across an interface between two density-stratified fluids have many applications including forecasting the water quality of reservoirs and controlling the efficiency of solar-ponds. Past experiments have been undertaken from the standpoint that turbulence in two-layered flows plays an important role in the entrainment phenomena. Rouse and Dodu (11) first used an oscillating-grid as a simple way to study the effect of turbulence. Turner (15) and Thompson and Turner (13) investigated the characteristics of turbulence by the use of a vertically oscillating grid and showed that an entrainment coefficient E is dependent on a local Richardson number Ri. The non-dimensional quantities E and Ri are defined as

$$E = u_e / u \qquad \text{and} \qquad Ri = (\rho_2 - \rho_1) g l / \rho_2 u^2$$

where u_e is the entrainment velocity, u and l are the horizontal intensity and integral lengthscale of turbulence at the interface, ρ_1 and ρ_2 are the densities of the upper- and lower-fluids, and g is the acceleration of gravity. Hereafter, $(\rho_2 - \rho_1)/\rho_2$ is referred to as ϵ. Linden (9) studied the mechanism of entrainment on the basis of simplified experiments involving one vortex-ring colliding against

an interface, and proposed an entrainment model $E \propto Ri^{-3/2}$. Hopfinger and Toly (3) obtained the relationship between the turbulence quantities and the conditions of grid oscillation by varying the dimensions of the grid. Ura, Komatsu and Matsunaga (19) revealed the mechanism of entrainment induced by an oscillating grid with the aid of flow visualization. Their entrainment data also supports the empirical relationship $E \propto Ri^{-3/2}$. Xuequan and Hopfinger (21) measured the entrainment velocity for both two-layered and constant-gradient stratified fluid systems with the oscillating-grid turbulence. They obtained $E = 3.8\ Ri^{-3/2}$.

Asaeda and Tamai (1) investigated the phenomena of entrainment in a two-layered stratified fluid. Their purpose was to discuss the relationships between variously defined entrainment coefficients and Richardson numbers. In their experiments, turbulence was generated by oscillating horizontally a bottom plate with prismatic roughness elements. They showed that the relationship of -3/2 power is seen between E and Ri defined by using the intensity of vertical component of turbulence velocity instead of u.

In two-layered flows having a mean shear, it has been common to describe the entrainment velocity by using bulk parameters of the flow rather than turbulence quantities. The velocity U_m averaged over water depth h of the mean flow or the friction velocity u_* have been used as an overall velocity scale and h as an overall lengthscale. Suga (12) experimented with a saline wedge and obtained the relation

$$E_m = 2.0 \times 10^{-3}\ Ri_m^{-3/2} \tag{1}$$

considering the data by Ellison and Turner (2), Lofquist (10) and Kato and Phillips (6). Here

$$E_m = u_e/U_m \qquad \text{and} \qquad Ri_m = \epsilon g h/U_m^2$$

However, scatter extended over one order in magnitude of E_m between Eq. 1 and their results. Kato and Phillips (6) and Kantha, Phillips and Azad (4) carried out experiments in which shear stress was applied to a water surface by rotating a screen. They considered that the entrainment velocity was closely related to the momentum added externally to stratified fluids, and they selected u_* acting on the water surface as the overall velocity scale. The resulting entrainment coefficient $E_*(= u_e/u_*)$ was not expressed as a simple power law of the overall Richardson number $Ri_*(=\epsilon g h/u_*^2)$.

The entrainment velocity was measured by Wu (20), Kit, Berent and Vajda (7), Ura ((16),(17)) and Kranenburg (8) for the case when wind shear stress acts on the water surface of a two-layered system. Wu and Kranenburg obtained the relation

$$E_* \propto Ri_*^{-1} \tag{2}$$

and Kit et al. and Ura proposed

$$E_* \propto Ri_*^{-3/2} \tag{3}$$

However, it should be noted that there is no remarkable difference between the data plotted by them, and that the exponents of Ri_* depend on their intuitions. In order to compare the entrainment velocity induced by wind shear stress with Eq. 1, Ura (17) plotted E_m against Ri_m by using for U_m the uniform velocity of a compensating return flow forming above the interface (see Fig. 3). He obtained the relation (see also Fig. 7)

$$E_m = 5.0 \times 10^{-2}\ Ri_m^{-3/2} \tag{4}$$

A comparison with Eq. 1 indicates that the velocity of entrainment by wind shear stress is about twenty five times as large as that by shear flow without wind.

We can know from the above references that many different expressions have been proposed for the entrainment coefficient for two-layered stratified flows. However, it is apparent that turbulence near an interface is essential in the

entrainment process, and that in order to obtain a unified expression for the entrainment velocity the analysis must be in terms of the turbulent velocity and lengthscale. Overall quantities such as U_m and u_* can not serve this purpose, not even existing in the case of turbulence entrainment induced by an oscillating grid.

This paper is concerned with an attempt to derive a general expression for the entrainment coefficient for two-layered flows. With this objective, four series of experimental investigations have been undertaken involving diverse modes of turbulence generation.

EXPERIMENTS

In order to determine the effect of turbulence on the entrainment velocity, experiments have been performed in four types of two-layered flows with stable stratification. These four cases are respectively characterized by oscillating-grid turbulence, a two-layered system with flow induced in the upper layer, and wind-induced flows with and without surface waves. The two layers consist of fresh and salt waters. The streamwise horizontal component of turbulent velocity has been measured with a hot-film anemometer. A 4-pole conductivity probe has been used for measuring the fluid density. By moving the conductivity probe vertically, density profiles have been obtained at 40 second intervals. The position of an interface is defined as the location where the mean fluid density is equal to $(\rho_1+\rho_2)/2$, and the entrainment velocity u_e has been estimated from time variations in the depth h from the water surface to the interface level (u_e = dh/dt).

Oscillating-Grid Turbulence

The measurements involving turbulence generation by an oscillating grid were performed by using a water tank shown schematically in Fig. 1. This tank was 1.00 m long, 0.254 m wide and 0.40 m deep. The turbulence was generated in the tank filled with homogeneous fresh water by oscillating a square grid vertically. Its mesh size M was 5.0 cm and the width d of the square bar 1.0 cm. Strokes S_0 of the grid oscillation were 1.0, 4.0 and 8.0 cm, and frequencies f_0 ranged from 1.5 to 6.0 Hz. The scotch-crank system was used to generate the sinusoidal oscillation. A lid was placed on the water surface to prevent undesirable fluctuations.

The hot-film probe was attached to a motor-driven carriage. The anemometer was calibrated by varying the carriage speed from 2.28 to 15.4 cm/s. The carriage

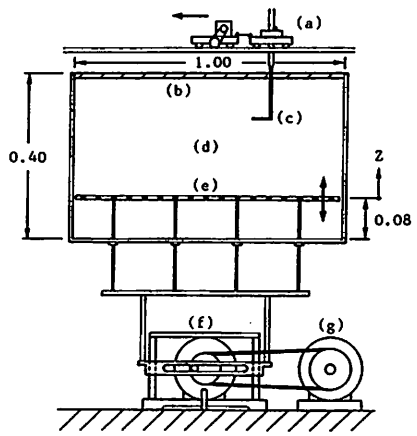

Fig. 1. Experimental apparatus for oscillating-grid turbulence (dimensions in m). Arrow indicates the direction of carriage motion and double arrow the direction of oscillation. (a) Carriage; (b) lid; (c) hot-film anemometer probe; (d) homogeneous working fluid; (e) square grid; (f) Scotch-crank; (g) helical geared motor.

speed was fixed at 8.29 cm/s during the measurement of turbulent velocity. Every measurement was repeated five times for each value of z, which indicates the distance measured upward from the mean position of the oscillating grid. The turbulence quantities were represented by the average values of five measurement series for each z.

Another small tank 0.254 m long was used for the measurement of entrainment velocity. A grid had the same mesh size and bar dimension as those above. The upper fresh-water layer was stirred by oscillating the grid. The values of S_0 and f_0 ranged from 1.0 to 4.0 cm and from 2.2 to 5.0 Hz, respectively. The density interface was set initially at $-2.20 \geqslant z \geqslant -15.3$ cm, and the initial values of ϵ were varied between 6.0×10^{-4} and 8.3×10^{-2}.

Upper-Layer Flow

Experiments were carried out by using the flume illustrated in Fig. 2. The flume was 6.0 m long, 0.3 m deep and 0.26 m wide, and its bottom was horizontal. Two kinds of fluid were introduced into the flume from constant head tanks. A porous pipe on the bottom permitted the slow introduction of salt water uniformly along the flume bed. A rigid guiding plate 1.0 m long was attached horizontally at the upstream end of the flume and at 0.15 m elevation from the bottom so as to avoid undesirable strong mixing between the upper and lower fluids. An outlet was designed at the downstream end in order to reduce the reflection of interfacial waves and the development of a layer with intermediate density. An upper-layer flow was set up by pouring a constant volume of fresh water on salt water stored previously in the flume. Three valves were adjusted to make the flow field stationary during the measurement of turbulent velocity.

Vertical distributions of the streamwise component of velocity were measured at distances 2.75 m downstream from the end of the guiding plate. Here let z be the vertical coordinate measured upward from the interface. The supply of salt water was stopped after the velocity measurement, and the deepening velocity of interface,i.e., the entrainment velocity, was measured. The value of Ri_a was varied from 1.90 to 9.18.

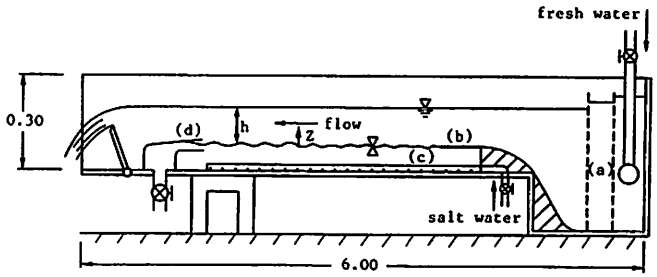

Fig. 2. Experimental apparatus for upper-layer flow (dimensions in m). (a) Fine mesh screens; (b) guiding plate; (c) porous pipe; (d) outlet.

Wind-Induced Flow with Surface Waves

The wind-wave flume used in this experiment is diagramed in Fig. 3. It was 5.0 m long, 0.20 m wide and 0.59 m high. The wind tunnel was 0.20 m high with an approach section 1.0 m long. A fetch of the wind over the water was 4.0 m. The flume was filled with a two-layered fluid where the initial value of ϵ varied from 4.0×10^{-4} to 5.4×10^{-2} and that of h was 0.1 or 0.2 m. The ordinate z is taken vertically upward from the mean water surface. Shear stress acted on the free water surface when the air blew into the tunnel, causing a drift current and compensating return flow as sketched in Fig. 3. Measurements of velocity were made at the center of the flume. To obtain the mean gradient of the interface, density profiles were measured at three positions which were at the distances 1.42, 2.42 and 3.40 m from the upstream end of the flume. Wind velocity was measured by using a two-component hot-wire anemometer and air friction velocity u_{*a}

was calculated from both the log-law applied to mean velocity profile and Reynolds stress. The values obtained from this two methods agreed closely. The vertical velocity distributions of the wind-induced flow were measured in the range $11.2 \leqslant u_{*a} \leqslant 58.3$ cm/s. The friction velocity u_* was evaluated from the relation

$$\rho_l u_*^2 = \gamma \rho_a u_{*a}^2$$

where ρ_a is the density of air, and γ was calculated based on the non-uniform flow model by using the measured mean gradient of the interface. The coefficient γ was found to have values between 1.0 and 0.9 (see, for example, (17)).

Wind-Induced Flow without Surface Waves

The experimental methods were almost the same as those described in the preceding section, except that a surfactant (sodium dodecyle sulfate, concentration 1.1×10^{-2} %) was added to the fresh and salt water in order to suppress the generation of surface waves. The initial values of ϵ and h were 7.8×10^{-3} and 0.2 m, respectively. The air friction u_{*a} ranged from 17.3 to 42.2 cm/s. The value of γ is 1.0 since no surface waves were generated.

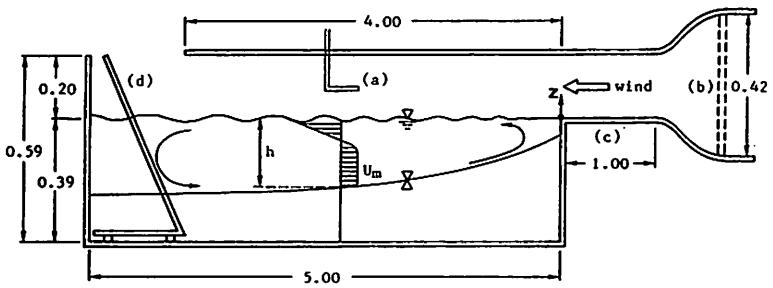

Fig. 3. Experimental apparatus for wind-induced flow (dimensions in m). (a) Hot-wire anemometer; (b) fine mesh screen; (c) approach section; (d) wave filter.

CHARACTERISTICS OF TURBULENCE

The intensity u and the integral lengthscale l of turbulence have been introduced as characteristic quantities. The lengthscale has been calculated on the basis of either the auto-correlation of the turbulent velocity or the empirical formula proposed by Townsend (14)

$$l = 0.8\, u^3 / \epsilon_d$$

Here ϵ_d is the rate of energy dissipation calculated from the -5/3-power law of wavenumber spectrum.

Oscillating-Grid Turbulence

The turbulence intensity has been calculated from $u=(\overline{u'^2}-\overline{u_0^2})^{1/2}$, because of the very weak correlation between the obtained turbulent velocity u' and the velocity irregularities u_0 due to the moving probe. The characteristic quantities u and l depend on M, f_0, S_0 and z since d/M = 0.2. Therefore, the non-dimensional relations

$$u/f_0 S_0 = f_1(z/M,\ S_0/M) \qquad \text{and} \qquad l/M = f_2(z/M,\ S_0/M)$$

are derived, and those for homogeneous fluids are shown with open marks in Figs.

4(a) to (c). We obtain the equations

$$\left.\begin{aligned} u/f_0S_0 &= 0.20\ (S_0/M)^{1/2}\,(z/M)^{-1} \\ l/M &= 0.14\ z/M \end{aligned}\right\} \qquad (5)$$

and find that l/M is independent of S_0/M.

Thompson and Turner (13) used the values of u and l obtained in a homogeneous fluid instead of those in a two-layered system because of the difficulty of keeping the stratified field stationary. It is necessary to demonstrate whether their idea is reasonable or not before we apply Eq. 5 to the two-layered field. In order to examine the effect of buoyancy on the characteristics of turbulence, a stationary two-layered field with strong buoyancy ($\varepsilon = 0.0284$) was formed in the tank shown in Fig. 1 by pouring salt and fresh waters into lower- and upper-layers, and by draining diluted salt water from the lower layer. The turbulent velocity was measured in this stationary field. The values u and l so determined are shown with a solid mark in Figs. 4(a) to (c). We find that these values compare well with Eq. 5 in the turbulent lower layer, though u and l damp rapidly after the turbulence has reached the interface. Therefore, we will estimate u and l for the turbulent layer of the two-layered field from Eq. 5.

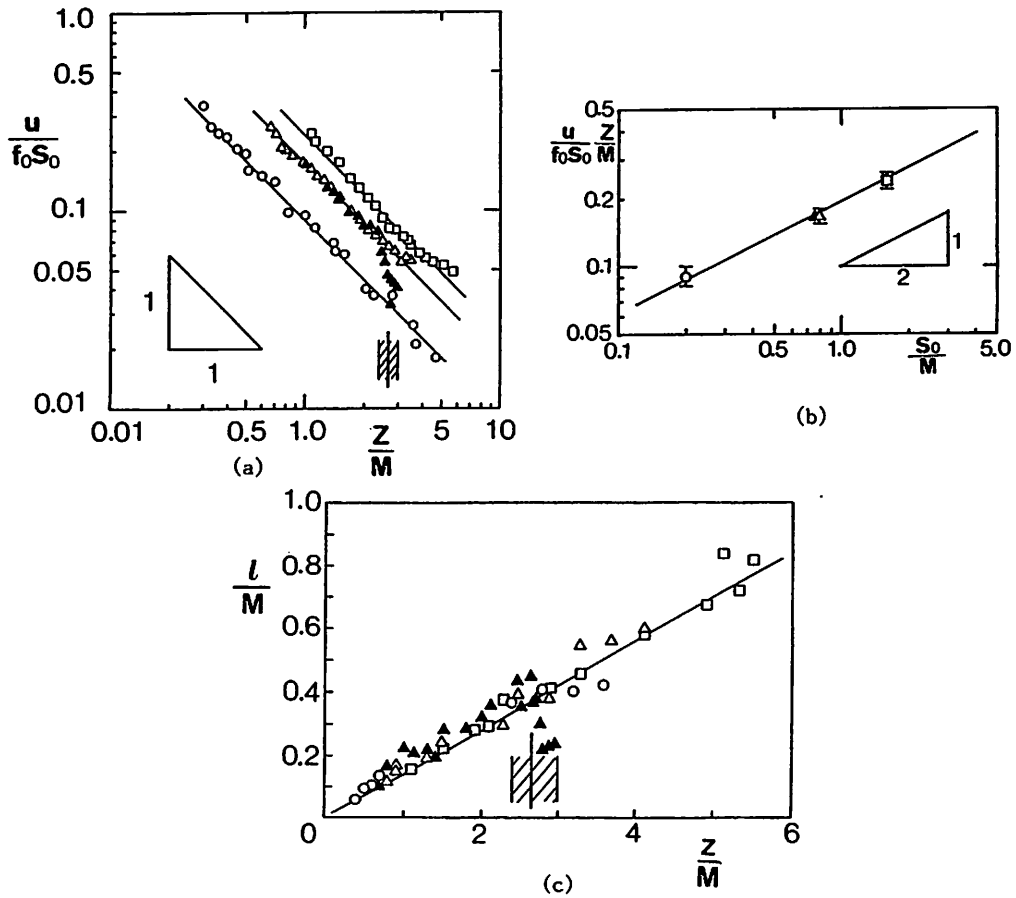

Fig. 4. Characteristics of oscillating-grid turbulence : ○, $S_0/M = 0.2$; △, $S_0/M = 0.8$; □, $S_0/M = 1.6$ in homogeneous fluid and ▲, $S_0/M = 0.8$ in two-layered fluid; The width of hatched region indicates the thickness of interface and solid line in this region shows the mean position of interface. (a) z/M-dependence of u/f_0S_0; (b) S_0/M-dependence of $(u/f_0S_0)(z/M)$; (c) z/M-dependence of l/M.

Upper-Layer Flow

Figs. 5(a) and (b) show the vertical distributions of u/U_m and l/δ_m in upper-layer flows. Here δ_m is the thickness of the interfacial boundary layer defined as $U_m/(dU/dz)_{z=0}$. The distributions of u/U_m take maximum values of about 0.1 for various values of Ri_m near the interface. We will use the maximum values as the characteristic intensity. The value of l/δ_m increases linearly with z/δ_m near the interface and the relation

$$l = \delta_m \qquad \text{at} \quad z = 0 \tag{6}$$

is obtained(see also (18)). The ratio of l to h was within the range from 0.15 to 0.31.

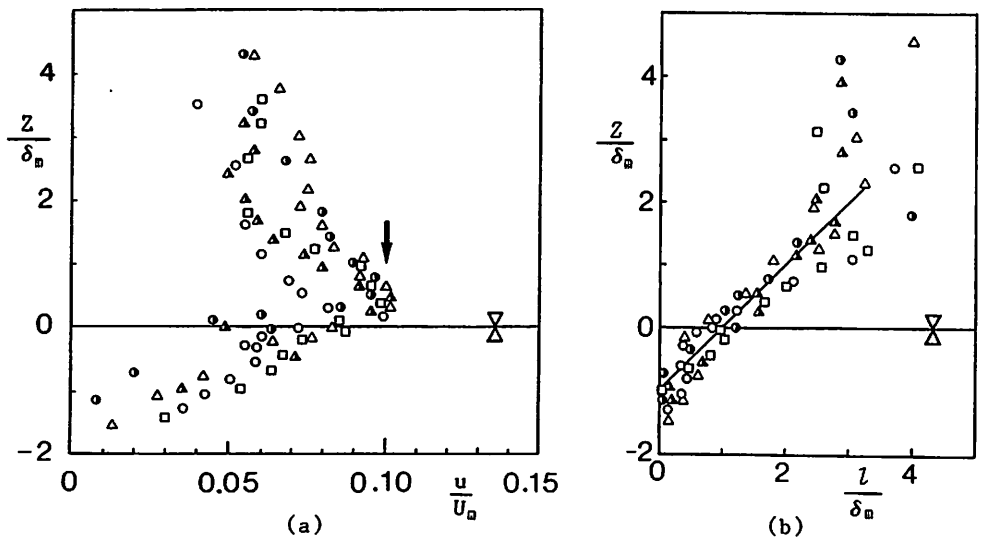

Fig. 5. Vertical distributions : ○, Ri_m = 2.36; △, Ri_m = 3.44; □, Ri_m = 4.27; ◑, Ri_m = 6.07; ▲, Ri_m = 9.18. (a) Intensity (arrow indicates the averaged maximum value); (b) integral lengthscale.

Wind-Induced Flow with and without Surface Waves

Figs. 6(a) and (b) show vertical distributions of mean velocity, turbulence intensity and integral lengthscale respectively for the cases with and without surface waves. A strong drift current is induced near the water surface by the wind, and return flow with a uniform velocity occurs in the range $-1.0 \leqslant z/h \leqslant -0.25$. It is found that U/u_* in the region of the return flow equals about 1.85 in both cases with and without the surface waves. Therefore, U_m is expressed by $1.85u_*$ when U_m denotes the uniform velocity of the return flow. The values of u/u_* are also constant in the return flow region, and the intensities are given by

$u = 0.65\ u_* = 0.35\ U_m$ for the case with surface waves, and
$u = 0.39\ u_* = 0.21\ U_m$ for the case without surface waves.

The integral lengthscales near the interface are given by

$l = 0.35$ h for the case with surface waves, and
$l = 0.20$ h for the case without surface waves,

though considerable scatter is seen in the distributions. It is seen that the characteristics of turbulence near the interface depend on whether surface waves form or not.

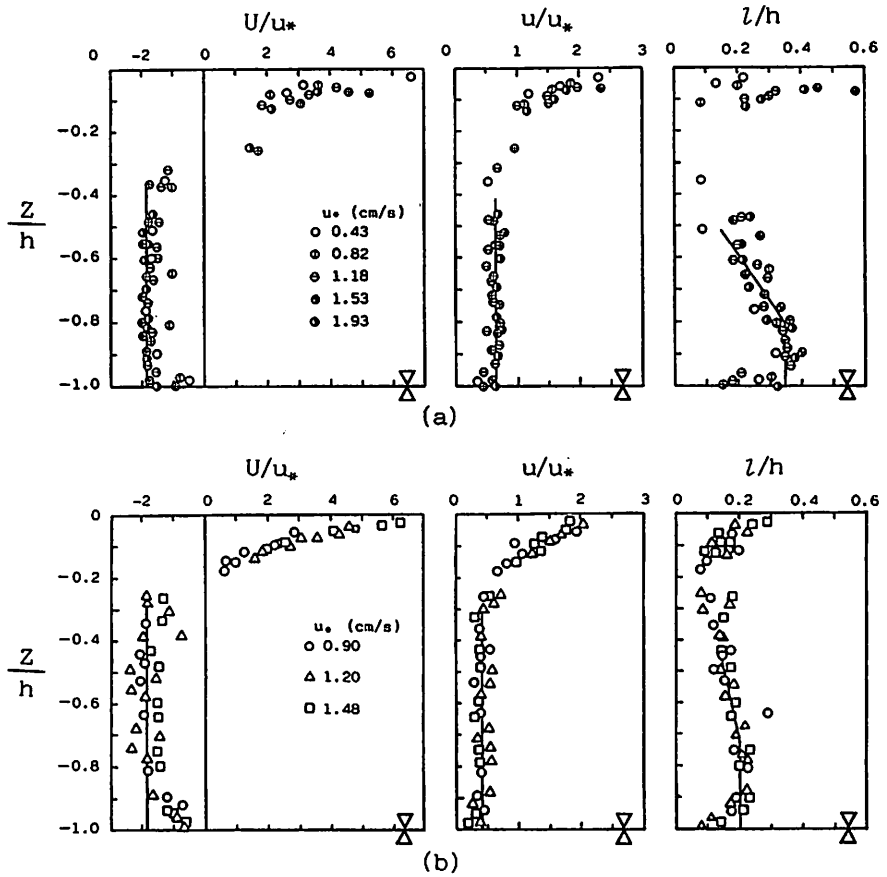

Fig. 6. Vertical distributions of mean velocity, turbulence intensity and integral lengthscale : (a) Case with surface waves; (b) case without surface waves.

ENTRAINMENT COEFFICIENT

The values of E_m for the upper-layer flow and the wind-induced flows are plotted against Ri_m in Fig. 7. The coefficient E_m in each flow field is approximately proportional to $Ri_m^{-3/2}$, but the proportional factor for the wind-induced flow with surface waves becomes twenty five times larger than that for the upper-layer flow. We find that even for the three types of flows it is impossible to express the entrainment coefficient universally only by plotting E_m against Ri_m.

As discussed earlier, the only approach to obtain a general expression for the entrainment coefficient is to consider the characteristic quantities of the turbulence. This is done in Fig. 8 where the coefficient $E = u_e/u$ is plotted against $Ri = \varepsilon g l/u^2$ for the four types of two-layered flows examined here as well as for the lower-layer flow measurements of Kato and Ikeda (5). Since Kato and Ikeda gave mean velocities and turbulence intensities except for integral lengthscales, they have been estimated by using Eq. 6. From these data we obtain a unified relationship between E and Ri,

$$E = 0.7\ Ri^{-3/2} \qquad (7)$$

It should be noted that Asaeda and Tamai's (1) data could not be plotted in this figure since the position of interface with respect to the measuring points of turbulent velocity was unclear in their paper.

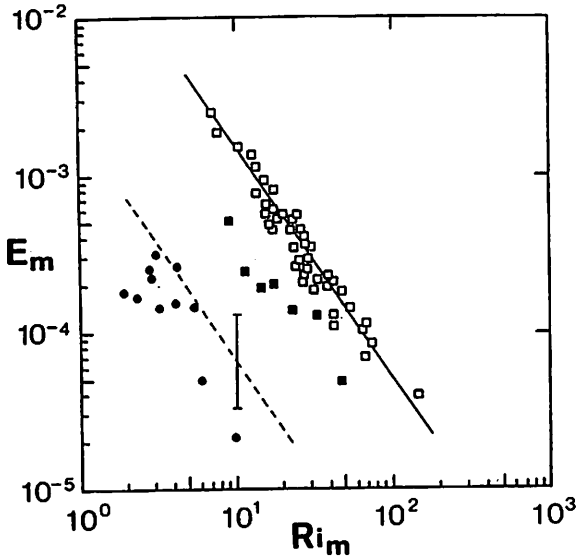

Fig. 7. Ri_m-dependence of E_m. Symbol ●, upper layer flow; □, wind-induced flow with surface waves; ■, wind-induced flow without surface waves; - - -, Eq. 1; ——, Eq. 4. The error bar indicates two times standard deviation about the mean line.

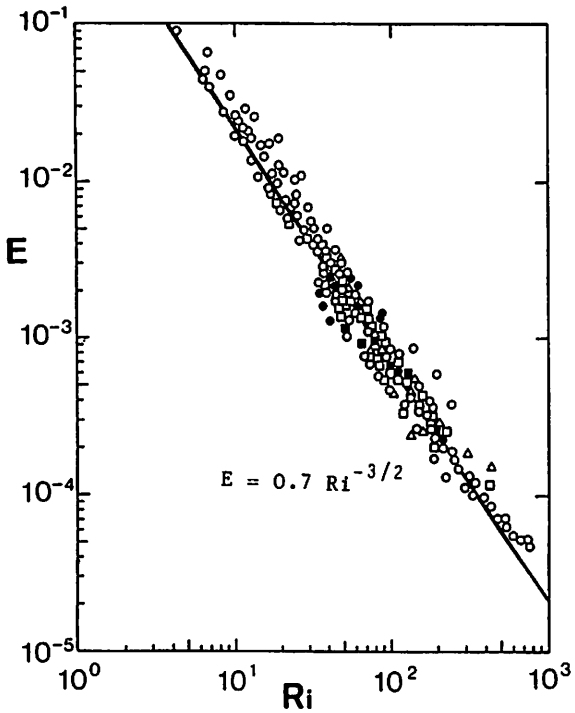

Fig. 8. Ri-dependence of E. Symbol ○, oscillating-grid turbulence; ●, upper-layer flow; □, wind-induced flow with surface waves; ■, wind-induced flow without surface waves; △, lower-layer flow by Kato and Ikeda(5); ——, Eq. 7.

Finally, we would like to stress the following. If Eq. 7 is rewritten by using the overall quantities (i.e. U_m and h), it becomes

$$E_m = u_e/U_m = 0.7(u/U_m)^4(l/h)^{-3/2}\, Ri_m^{-3/2}$$

This indicates that Eq. 7 is compatible with the relation $E_m \propto Ri_m^{-3/2}$ shown in Fig. 7 and that the difference between proportional factors seen in Fig. 7 is due to that of the characteristic quantities of turbulence.

The authors thank Dr T.Komatsu and Prof. P.D.Komar for stimulating discussions and Mr N.Nakashiki for technical help.

REFERENCES

1. Asaeda, T. and N. Tamai : Turbulent entrainment in stratified flow, Proc. 3rd Int. Symp. on Stochastic Hyd., pp.445-456, 1980.
2. Ellison, L.H. and J.S. Turner : Turbulent entrainment in stratified flows, J. Fluid Mech., Vol.6, pp.423-448, 1959.
3. Hopfinger, E.J. and J.A. Toly : Spatially decaying turbulence and its relation to mixing across density interface, J. Fluid Mech., Vol.78, pp.155-175, 1976.
4. Kantha, L.H., O.M. Phillips and R.S. Azad : On turbulent entrainment at a stable density interface, J. Fluid Mech., Vol.79, pp.753-768, 1975.
5. Kato, H. and T. Ikeda : An experiment of lower density current (1) -velocity profile and entrainment coefficient-, The 28th Japanese Conf. Coastal Eng., pp.520-524, 1981(in Japanese).
6. Kato, H. and O.M. Phillips : On the penetration of a turbulent layer into stratified fluid, J. Fluid Mech., Vol.37, pp.643-655, 1969.
7. Kit, E., E. Berent, and M. Vajda : Vertical mixing induced by wind and a rotating screen in a stratified fluid in a channel. J. Hyd. Res., Vol.18, No.1, pp.35-58, 1980.
8. Kranenburg, C. : Mixed-layer deepening in lakes after wind setup, J. Hyd. Eng., ASCE, Vol.111, No.9, pp.1279-1297, 1985.
9. Linden, P.F. : The interaction of a vortex ring with a sharp density interface, a model for turbulent entrainment, J. Fluid Mech., Vol.160, pp.467-480, 1973.
10. Lofquist, K. : Flow and stress near an interface between stratified liquids, Phys. Fluids, Vol.3, pp.158-175, 1960.
11. Rouse, H. and J. Dodu : Turbulent diffusion across a density discontinuity, La Houille Blanche, No.10, pp.530-532, 1955.
12. Suga, K. : Unsteady, stratified flow with entrainment by tides, Proc. IAHR., Vol.A-37, pp.287-294, 1977.
13. Thompson, S.M. and J.S. Turner : Mixing across an interface due to turbulence generated by an oscillating grid, J. Fluid Mech., Vol.67, pp.349-368, 1975.
14. Townsend, A.A. : The Structure of Turbulence Shear Flow,(2nd ed.), Cambridge University Press, 1976.
15. Turner, J.S. : The influence of molecular diffusivity on turbulent entrainment across a density interface, J. Fluid Mech., Vol.33, pp.639-656, 1968.
16. Ura, M. : Interfacial waves and entrainment velocity across the density interface under the action of the wind stress, Proc. 30th Japanese Conf. Coastal Eng., pp.561-565, 1983. (in Japanese).
17. Ura, M. : Interfacial waves and entrainment in a wind-induced stratified flow, Proc. 4th Cong. APD-IAHR, pp.403-417, 1984.
18. Ura, M., T. Tsubaki and N. Matsunaga : Characteristics of flow and turbulence near interfacial waves in upper-layer flow, J. Hydro. and Hyd. Eng., Vol.2, No.1, pp.27-45, 1984.
19. Ura, M., T. Komatsu and N. Matsunaga : Entrainment due to oscillating-grid turbulence in two-layered fluid, Turbulence Measurements and Flow Modeling, Springer-Verlag, pp.109-118, 1987.
20. Wu, J. : Wind-induced turbulent entrainment across a stable density interface, J. Fluid Mech., Vol.61, pp.275-287, 1973.
21. Xuequan, E. and E.J. Hopfinger : On mixing across an interface in stably stratified fluid, J. Fluid Mech., Vol.166, pp.227-244, 1986.

APPNDIX — NOTATION

The following symbols are used in this paper:

- d = width of square bar of an oscillating grid;
- E = entrainment coefficient defined by u_e/u;
- E_m = entrainment coefficient defined by u_e/U_m;
- E_* = entrainment coefficient defined by u_e/u_*;
- f_o = frequency of grid oscillation;
- g = acceleration of gravity;
- h = depth of turbulent layer;
- l = integral lengthscale of turbulence;
- M = mesh size of an oscillating grid;
- Ri = local Richardson number defined by $\epsilon g l/u^2$;
- Ri_m = overall Richardson number defined by $\epsilon g h/U_m^2$;
- Ri_* = overall Richardson number defined by $\epsilon g h/u_*^2$;
- S_o = stroke of grid oscillation;
- t = time;
- u = horizontal intensity of turbulence;
- u' = turbulent velocity;
- u_e = entrainment velocity;
- u_o = velocity irregularity due to the moving probe;
- u_* = friction velocity;
- u_{*a} = air friction velocity;
- U = mean velocity;
- U_m = velocity averaged over turbulent layer;
- z = vertical distance from the mean position of the oscillating-grid (in the case of oscillating-grid turbulence);
  = vertical coordinate measured above from interface (in the case of upper-layer flow);
  = vertical coordinate taken vertically upward from free water surface (in the case of wind-induced flow);
- γ = coefficient of stress transfer at water surface;
- δ_m = thickness of the interfacial boundary layer defined by $U_m/(dU/dz)_{z=0}$;
- ϵ = non-dimensional density difference defined by $(\rho_2 - \rho_1)/\rho_2$;
- ϵ_d = rate of energy dissipation;
- ρ_a = density of air;
- ρ_1 = mean density of upper-layer fluid; and
- ρ_2 = mean density of lower-layer fluid.